Peristaltic patterns for swelling and shrinking of soft cylindrical gels

Pasquale Ciarletta[a†] **and Martine Ben Amar**[b]

Received Xth XXXXXXXXXX 20XX, Accepted Xth XXXXXXXXX 20XX
First published on the web Xth XXXXXXXXXX 200X*, DOI: 10.1039/b000000x*

We propose a variational method for determining the surface patterns of cylindrical gels for both swelling and shrinking. Exact solutions are calculated for the initial stages of such peristaltic instabilities. The morphology and the formation mechanisms depend on a competition between bulk elastic energy and surface tension.

The emergence of complex spatio-temporal patterns in growing gels has been the object of a number of physico-chemical studies in the last years[1]. Indeed, polymeric gels are very soft elastic materials, which can undergo a volume phase transition when a small change of an external parameter, like temperature or solvent concentration, occurs. Pioneering experimental works of Tanaka and coworkers[2] have demonstrated that such volume variations, once geometrically constrained, generate residual stresses inside the material, which can eventually trigger an elastic instability. Thanks to the high controllability of the experimental systems, investigations on swelling or shrinking of polymeric gels are used for understanding the morphogenetic processes in soft biological matter, other than guiding smart surface fabrication and biomaterial design.

In cylindrical gels, the surface patterns arising in swelling and shrinking processes differ in both their morphology and their formation mechanism. For swelling gels, incompatible growth may result in a compressive strain driving a short-wavelength buckling of the free surface, a mechanical instability first reported by Biot[3] for rubbers. In contrast, Matsuo and Tanaka[4] experimentally observed different types of shrinking patterns. The appearance both of regularly spaced collapsed gel planes (bamboo pattern) and of surface wrinkles (wrinkled tube pattern) in the cylindrical gel was qualitatively explained by different mechanisms of spinodal decomposition. The spontaneous formation of alternated domains of collapsed and swollen phases (bubble pattern), first interpreted by a phase separation, was later explained as a capillary-driven instability[5]. The origin of such a peristaltic modulation of the gel surface is similar to the Rayleigh-Plateau instability of a liquid jet, characterized by a long wavelength undulation reducing the surface area while retaining the volume. In the case of a soft gel, bubble formation during shrinking is a more complicated and less understood mechanism, driven by the competition between surface tension and elastic bulk properties of the cylinder. *Moreover, experiments on acrylate-acrylamide gels in water-acetone mixture have demonstrated that a mechano-chemical coupling can drive the formation of different patterns*[6]*. Bubbles are observed if the gel is shrunk almost homogeneously, while rings (longitudinal wrinkles) appear if a mechanical compression (elongation) is imposed.*

In this study, we aim at proposing a unified modeling for both swelling and shrinking soft gels, deriving exact solutions for the initial stages of both types of peristaltic instabilities.

We consider a soft cylinder with initial radius R_o and axial length L, confined at its lateral surfaces (z=0,L) by rigid walls, preventing any longitudinal sliding. A homogeneous growth process takes place in each point of the cylinder, so that locally any volume element increases by a constant factor J. Such a growth process, also referred as volumetric growth, is described now by the so-called multiplicative decomposition of the deformation gradient $\mathbf{F} = \mathbf{F}_e\mathbf{F}_g$[7], setting a homogeneous, anisotropic form for the growth tensor, which in polar coordinates reads $\mathbf{F}_g = \mathrm{diag}(g_r, g_r g_\theta, g_z)$, J being simply $J = \det\mathbf{F}_g = g_r^2 g_\theta g_z$ and $\mathbf{F}_e$ the elastic strain tensor. For initially full cylinders we must set $g_\theta = 1$ in order to avoid singularities at $R = 0$. We assume that the soft cylinder behaves as a neo-Hookean material, which is the entropic elasticity of polymeric gels, so that the elastic energy per unit volume Ψ is

$$\Psi_{iso} = J \cdot \frac{\mu}{2}(\mathrm{Trace}(\mathbf{F}_e^T\mathbf{F}_e) - 3) - p \cdot (\det\mathbf{F}_e - 1) \qquad (1)$$

where μ is the shear modulus and p, like the pressure in hydrodynamics, is the classical Lagrange multiplier ensuring the incompressibility of the gel.

For an isotropic growth process with $g_r = g_z = g$, where $g > 1 (g < 1)$ for gel swelling (shrinking), an obvious homogeneous elastic solution is given by a constant expansion (contraction) of the radius $r = g^{3/2}R = \sqrt{J}R$, with $\theta = \Theta$, $z = Z$. Nevertheless such a radial expansion (contraction) is responsible for a compressive (tensile) stress in the longitudinal direction (in our case the cylinder axis) and one can expect the occurrence of a bifurcation as the growth rate g increases (decreases). To do so, and to respect the incompressibility of the sample, we introduce a scalar generating function $\Phi(R,\theta, z)$ in

† Corresponding author (ciarletta@dalembert.upmc.fr)
[a] *CNRS & Institut Jean le Rond d'Alembert, UMR7190, Place Jussieu 4, Case 162, 75005 Paris, France*
[b] *Laboratoire de Physique Statistique, Ecole Normale Supérieure, UPMC Univ Paris 06, Université Paris Diderot, UMR CNRS 8550, 24 rue Lhomond, 75005 Paris, France*

mixed coordinates in order to build arbitrary isochoric transformations. Such function, equivalent to the stream function used in hydrodynamics, solves exactly the incompressibility condition, having the following gradient form:

$$\mathrm{r}^2 = 2\,\Phi_{,\mathrm{Z}}; \qquad \mathrm{Z} = \frac{\Phi_{,\mathrm{R}}}{\mathrm{J\,R}}; \qquad \Theta = \theta \tag{2}$$

so that the elastic deformation gradient $\mathbf{F}_e$ can be rewritten as:

$$\mathbf{F}_{\mathrm{e}} = \begin{bmatrix} \frac{1}{g\sqrt{2\,\Phi_{,z}}}\left(\Phi_{,Rz} - \frac{\Phi_{,zz}\,(\Phi_{,RR}-\Phi_{,R}/R)}{\Phi_{,Rz}}\right) & \frac{g^2\,R\,\Phi_{zz}}{\sqrt{2\,\Phi_{,z}}\,\Phi_{,Rz}} & 0 \\ -\frac{\Phi_{,RR}-\Phi_{,R}/R}{g\Phi_{,Rz}} & \frac{g^2\,R}{\Phi_{,Rz}} & 0 \\ 0 & 0 & \frac{\sqrt{2\,\Phi_{,z}}}{gR} \end{bmatrix} \tag{3}$$

and the incompressibility constraint $\det\mathbf{F}_{\mathrm{e}} = 1$ is identically satisfied. In absence of external body forces and surface loads, the elastic boundary value problem is equivalent to the minimization of the total stationary energy Π of the cylinder, which can be written as follows:

$$\delta\Pi = \delta\left(\int_{\bar{\Omega}_z} \bar{\Pi}_z d\bar{\Omega}_z\right) = \delta\left(J^{-1}\int_{\bar{\Omega}_z} \Psi_{iso}\Phi_{,\mathrm{Rz}}\mathrm{dR}\,\mathrm{d\theta}\,\mathrm{dz}\right) = 0 \tag{4}$$

where $\bar{\Omega}_z$ is the body volume in the intermediate mixed configuration. The Euler-Lagrange equation, valid everywhere inside the cylinder and solving Eq.(4), using Einstein's convention for summation reads:

$$\left(\frac{\partial\bar{\Pi}_z}{\partial\Phi_{,ij}}\right)_{,ij} - \left(\frac{\partial\bar{\Pi}_z}{\partial\Phi_{,k}}\right)_{,k} = 0 \tag{5}$$

the index meaning either R or z. The two boundary conditions at the free surface $R = R_o$ are given by imposing minimization with respect to arbitrary variations on Φ and on $\Phi_{,R}$, as follows:

$$\frac{\partial\bar{\Pi}_z}{\partial\Phi_{,R}} - \left(\frac{\partial\bar{\Pi}_z}{\partial\Phi_{,RR}}\right)_{,R} - \left(\frac{\partial\bar{\Pi}_z}{\partial\Phi_{,Rz}}\right)_{,z} = 0;\ \frac{\partial\bar{\Pi}_z}{\partial\Phi_{,RR}} = 0 \tag{6}$$

and the two other boundary conditions impose regularity of the solution at $R = 0$.

In order to perform a linear stability analysis of our ideal homogeneous elastic solution, defined by $\Phi^0 = J(R^2)z/2$, we assume a tiny periodic longitudinal perturbation, giving the following expression of the scalar generating function:

$$\Phi(R,z) = \frac{J}{2}(R^2)z + \varepsilon\cdot u\left(\sqrt{J}R\right)\cdot\sqrt{J}R\cdot\cos\left(\mathrm{m}\frac{2\pi\mathrm{z}}{\mathrm{L}}\right) \tag{7}$$

where m is a positive integer and $|\,\varepsilon\,| \ll 1$. Using Eq.(7), the perturbation in Eq.(2) at the first order in ε can be rewritten in the following form:

$$\begin{cases} \mathrm{r} = \sqrt{\mathrm{J}}\mathrm{R} + \varepsilon\cdot\mathrm{k}\,\mathrm{u}\left(\sqrt{\mathrm{J}}\mathrm{R}\right)\cos(\mathrm{kz}) \\ \mathrm{Z} = \mathrm{z} + \varepsilon\cdot\left(\mathrm{u}'\left(\sqrt{\mathrm{J}}\mathrm{R}\right) + \frac{\mathrm{u}(\sqrt{\mathrm{J}}\mathrm{R})}{\sqrt{\mathrm{J}}\mathrm{R}}\right)\cdot\sin(\mathrm{kz}) \end{cases} \tag{8}$$

where we have introduced $k = 2\pi m/L$ (see Fig.1). Substituting the expression of Eq.(8) in Eq.(5), the bulk Euler-Lagrange equation at the first order in ε reads:

$$\mathcal{L}_1\mathcal{L}_J[u(r)] = 0 \text{ with } \mathcal{L}_Q = \left(\frac{\partial^2}{\partial r^2} + \frac{1}{r}\frac{\partial}{\partial r} - \frac{1}{r^2} - \frac{k^2}{Q}\right) \tag{9}$$

Note that $\mathcal{L}_1$ denotes the second order differential operator corresponding to the Laplacian in cylindrical coordinates and that both operators accept as eigensolutions the modified Bessel function of first order I_1 and K_1. Since only I_1 is regular for $r = R = 0$ the analytical solution of Eq.(9) is easily obtained by superposition, so that $u(r)$ reads:

$$u(r) = \alpha\left(\frac{I_1(kr/\sqrt{J})}{I_1(kr_o/\sqrt{J})} + \beta\frac{I_1(kr)}{I_1(kr_o)}\right) \tag{10}$$

At the same way, the Euler-Lagrange equation at the free surface $r_o = g^{3/2}R_o = \sqrt{\mathrm{J}}R_o$, from Eq.(6), take the following expressions:

$$\mathcal{B}_1[u(r)] = \mathcal{L}_1[u(r)] + 2k^2u(r) = 0 \tag{11}$$

$$\mathcal{C}_J[u(r)] = k^2r^2\,(ru)' + J\left[-u + ru' + 2k^2r^3u' - r\left(r^2u''\right)'\right] = 0 \tag{12}$$

Noticing that $\mathcal{L}_1I_1(kR) = k^2(1+J)/J$ and $\mathcal{L}_1I_1(kr) = 0$ one easily derive from the boundary condition in Eq.(11), the coefficient β in Eq.(10) as $\beta = -(\mathrm{J}+1)/(2\mathrm{J})$, α remaining arbitrary at linear order. The dispersion relation $\Omega(J)$ gives k as a function of g at threshold with $\Omega(J) = 0$. Found by substitution of Eq.(10) in the boundary condition given by Eq.(12), it reads:

$$\Omega(J) = 2 + \frac{kr_o}{J(J-1)}\left[(1+J)^2\frac{I_0(kr_o)}{I_1(kr_o)} - 4J^{3/2}\frac{I_0(kR_o)}{I_1(kR_o)}\right] \tag{13}$$

Plotting this implicit relation for $k, g > 0$, it is possible to show that the smallest value of g giving rise to an instability is obtained for k going to infinity, which is the typical behavior of a surface Biot instability[3]. In order to find this threshold value of growth, we can use the asymptotic relation $I_n(x) \sim e^x/\sqrt{2\pi x}$, valid for $x \gg 1$, in Eq.(13) and find the exact value for the threshold growth rate g_{th} giving rise this surface instability:

$$g_{th} = \left(\frac{11}{3} + \frac{2}{3}\cdot\left((199 - 3\sqrt{33})^{1/3} + (199 + 3\sqrt{33})^{1/3}\right)\right)^{1/3} \tag{14}$$

which is approximatively $\simeq 2.2534$ and higher than the one we derived for a growing gel layer attached to a fixed plane[8]. Being $\mathbf{e}_z$ is the unit vector in the longitudinal direction, the instability threshold is fixed by the longitudinal stretch $\lambda_z = |\mathbf{F}_e\mathbf{e}_z|$ inside the material. In our case, such a stretch is compressive, being given by $\lambda_z = 1/g^{th} \simeq 0.4437$, which corresponds

to the numerical result obtained by Vaughan[9]. However, there is a lack of a typical lengthscale to fix the undulation wavelength to a finite value. Such an instability costs a lot in surface energy and surface tension fixes the wavelength instability at threshold. Let A be the surface energy associated to a surface tension γ at r_o:

$$A = 2\pi\gamma \int r(z)\sqrt{1+r_{,z}^2}dz = 2\pi\gamma \int \sqrt{2\Phi_{,z}+\Phi_{,zz}^2}dz \quad (15)$$

Considering the competition between a bulk elastic energy density $\bar{\Pi}_z$ and the surface energy A, the variation problem reads $\delta A + \delta\Pi = 0$, which induces a change only in first of the two boundary conditions in Eq.(6), which becomes :

$$\frac{\partial\bar{\Pi}}{\partial\Phi_{,R}} - \left(\frac{\partial\bar{\Pi}}{\partial\Phi_{,RR}}\right)_{,R} - \left(\frac{\partial\bar{\Pi}}{\partial\Phi_{,Rz}}\right)_{,z} + \left(\frac{\partial A}{\partial\Phi_{,zz}}\right)_{,zz} - \left(\frac{\partial A}{\partial\Phi_{,z}}\right)_{,z} = 0 \quad (16)$$

Substituting Eq.(7) in Eq.(16), we find the correction of the boundary condition $\mathcal{C}_{J,\gamma}$ in Eq.(12) due to the capillarity :

$$\mathcal{C}_{J,\gamma}[u(r)] = \mathcal{C}_J[u(r)] + k^2\frac{\gamma g^2}{\mu}r(-1+k^2r^2)u(r) \quad (17)$$

where it appears a capillary length, given by $L_c = \gamma/\mu$, which intervenes in the dispersion relation of the instability, as follows:

$$\tilde{\Omega}(J) = \Omega(J) + \frac{\gamma}{g^{5/2}\mu R_0}(1 - Jk^2R_o^2) = 0 \quad (18)$$

First, from Eq.(18) it is possible to detect the occurrence of a capillary instability (at long wavelength, i.e. $k \ll 1$) if the following condition holds:

$$\gamma = 2\mu R_o\frac{(1+2g^3)}{g^{1/2}} \quad (19)$$

which in absence of growth ($g = 1$) recovers the static result for soft cylindrical gels[10]. The right hand side of Eq.(19) is a positive function having a minimum for $g = (1/10)^{1/3} \simeq 0.4641$, corresponding to $\eta_{min} = (L_c/R_o)_{min} = 12(2^{1/6}/5^{5/6}) \simeq 3.5227$. Therefore, we can state that the instability mechanism is characterized by the ratio between the capillary length L_c and the radius R_0: if $\eta = L_c/R_o \ll \eta_{min}$ one has a surface instability driven by a critical gel swelling ($g > 1$), while if $\eta \geq \eta_{min}$ a capillary instability is favored by the gel shrinking. Typical values of the capillary energy for soft polymeric gels are of the order of $35 - 70 \cdot 10^{-3} N/m$, while their shear modulus can range from tens to thousands of Pa[1], corresponding to a characteristic lengthscale $L_c \simeq 0.1 - 1mm$. The theoretical prediction of Eq.(19) is therefore in accordance with the experimental results of Matsuo and Tanaka[4]. For R_0 of the order L_c/η_{min}, the occurrence of bubble pattern can be triggered by the action of the surface tension, enhanced by the observed formation of a dense skin layer on deswollen gels, taking over the stabilizing effect of the bulk elasticity.

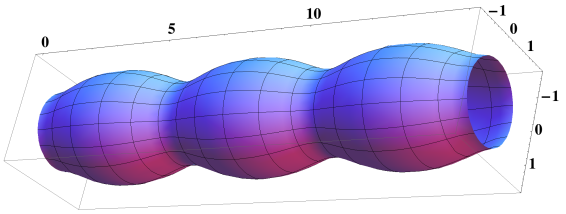

Fig. 1 Isochoric perturbation of a cylinder with L=15, R=1.5, ε=0.3.

Moving from the isotropic model of gels, now we analyze the instability accounting for the presence of fibers inside the cylinder. In fact, cylindrical structures in the biological realm (e.g. myelinated nerves) are often characterized by longitudinal fibers, undergoing stretch-induced beading in their physiological functions[11]. Taking into account a longitudinal fiber reinforcement, the anisotropic strain energy function can be modeled as follows[12]:

$$\Psi_{tot} = \Psi_{iso} + J\cdot\frac{K_1}{4}\cdot\left(\lambda_z - \lambda_z^{-1}\right)^2 \quad (20)$$

where K_1 is a material parameter determining the fiber stiffness, an λ_z indicates the longitudinal elastic stretch.
Substituting the expression of Eqs.(3, 7, 20) in Eq.(5), the bulk Euler-Lagrange equation at the first order in ε reads:

$$\mathcal{L}_1\mathcal{L}_{\bar{J}}[u(r)] = 0 \ \text{ with } \bar{J} = J\left(\mu + g\frac{K_1}{2}\right)/\left(\mu + \frac{K_1}{2}\right) \quad (21)$$

where $\mathcal{L}_{\bar{J}}$ denotes the same second order differential operator, $\bar{J}$ accounting for material anisotropy. We deduce immediately the general solution for the perturbed displacement $u(r)$ of Eq.(21), considered regular for $r = 0$, as :

$$u(r) = \alpha\left(\frac{I_1(kr/\sqrt{\bar{J}})}{I_1(kr_o/\sqrt{\bar{J}})} + \beta\frac{I_1(kr)}{I_1(kr_o)}\right) \quad (22)$$

by replacing J by $\bar{J}$, being $\beta = -(1+\bar{J})/(2\bar{J})$.
Only the boundary condition at the free surface $r_o = g^{3/2}R_o$, from Eqs.(6,16) is modified with J replaced by $\bar{J}$, $\mathcal{C}_{\bar{J},\gamma,K_1}$ taking the following expressions once surface tension and material anisotropy are taken into account:

$$\mathcal{C}_{\bar{J},\gamma,K_1}[u(r)] = \mathcal{C}_{\bar{J}}[u(r)] + \frac{k^2g^2r}{(\mu+\frac{K_1}{2})}\left(\gamma(-1+k^2r^2) - K_1rg^2\right)u(r) \quad (23)$$

As done before, we deduce without difficulty the dispersion relation substituting Eqs.(22) in the boundary condition given by Eq.(23), having the following simplified form:

$$0 = 2 + \frac{kr_0(1+\frac{K_1}{2\mu})}{J(\bar{J}-1)}\left[(1+\bar{J})^2\frac{I_0(kr_o)}{I_1(kr_o)} - 4\bar{J}^{3/2}\frac{I_0(\frac{kr_o}{\sqrt{\bar{J}}})}{I_1(\frac{kr_o}{\sqrt{\bar{J}}})}\right] + \frac{\gamma(1-k^2r_0^2)}{\mu g^{5/2}R_o} \quad (24)$$

Using the asymptotic expansion for $k \to \infty$, we can find a simplified dispersion relation for the surface instability. In particular, if γ/μ, $\gamma/K_1 \ll 1$, i.e. the capillarity is a local effect at the free surface, the growth threshold g_* of the surface instability is given by the following relation:

$$1+\bar{J}=2\bar{J}^{3/4};\ \text{or}\quad \mathrm{g}_*^3\cdot(\mu+\mathrm{g}_*\mathrm{K}_1/2)=(\mu+\mathrm{K}_1/2)\cdot\mathrm{g}_{\mathrm{th}}^3 \quad (25)$$

which states that the presence of an axial anisotropic reinforcement lowers the growth threshold g_* of the swelling instability. In particular, such a critical threshold is bounded by an upper level given by the isotropic case (g_{th}, when $c_1/K_1 \gg 1$), and a lower value given for $c_1/K_1 \ll 1$ by:

$$g_*^{min}=g_{th}^{3/4}\simeq 1.8392 \quad (26)$$

which is surprisingly the same threshold we found for the swelling of a surface-attached gel layer[8]. Finally, we investigate the occurrence of a surface instability looking at the limit of Eq.(24) for $k \to 0$, which is the case of shrinking. In that case, the threshold relation can be expressed as a function characteristic length-scales, as follows:

$$\eta_*=\frac{\gamma}{(\mu+\frac{K_1}{2})R_o}=\frac{\eta}{1+\frac{K_1}{2\mu}}=\frac{2}{\sqrt{g}}\left(1+2\bar{J}+\frac{K_1 g^4}{\mu+\frac{K_1}{2}}\right) \quad (27)$$

so that the minimum value η_* for the anisotropic case is greater than the one found in the isotropic case, while the threshold growth is almost unchanged. In particular, if $K_1 >> \mu$, the minimum threshold is determined by a growth rate $g_* = (1/21)^{1/4} \simeq 0.4671$, which gives $\eta^{min} \simeq 1.6721$. Compared to the isotropic case, the presence of a material anisotropy favors the occurrence of a swelling instability in Eq.(25), while has a stabilizing effect in shrinking, from Eq.(27), with respect to capillarity driven undulations. According to our theoretical predictions, the observed beading of nerve fibers can be interpreted as a peristaltic instability driven by the surface tension of their external membrane. Taking into account experimental values[11,13] of $K = 0.1-1$ MPa and $\gamma = 0.8$(unmyelinated)-2(myelinated fiber)N/m, the typical lengthscale $L_c \simeq 1-10\mu m$ is of the same order as the nerve radius $R \simeq 0.5-5\mu m$. Therefore applying an equivalent longitudinal stretch $\lambda_z = 1/g > 1$ to the nerve has the effect to lower the threshold value η_* in Eq.(27), possibly triggering the onset of a surface instability. Such a prediction of our model is supported by the long wavelength undulation and the reversibility of beading in experiments, occurring while stretching both myelinated and unmyelinated nerve filaments.

In this work, we have studied the formation of surface patterns observed for growing cylindrical gels. Using a nonlinear elastic analog of the stream function in hydrodynamics, *swelling and shrinking instabilities are found to be driven by competition between bulk elasticity and surface tension. The short-wavelength undulations in swelling are caused by residual deformations, while bubble-like patterns occur in shrinking cylindrical gels with a radius about the order of the capillary length.* We have calculated the exact solutions of the initial shapes of the undulations as well as the analytical thresholds for the instabilities. Although we predict the effects of homogeneous volume changes on the occurrence of peristaltic instability, we do not consider the gel-solvent dynamics, which in turn is found to fix the preferred wavenumber of the peristaltic pattern[14]. The proposed gel model has been finally used for studying pattern formation of soft fibrous cylinders, mimicking the beading instability of nervous filaments. *Fiber-reinforcements stabilize with respect to shrinking instabilities: the increase in elastic stiffness determines a decrease in the critical filament diameter which triggers the formation of surface undulations. A quantitative* understanding on how elasticity of the fibers and surface tension concur for promoting this beading instability can have an impact for the design of polymer nanofibers[15]. The control of the number and sizes of the beads in fabrication techniques is in fact a key aspect for a number of applications, from drug-delivery agents to soft tissue engineering. In conclusion, the proposed simultaneous treatment of elastic growth, surface tension and microstructure is of utmost importance both for understanding soft tissues morphogenesis and for applications in biomedical sciences.

References

1 J. Dervaux and M. Ben Amar, *Annu. Rev. Condens. Matter Phys.*, 2012, DOI: 10.1146/062910-140436

2 T. Tanaka, S.T. Sun, Y. Hirokawa, S. Katayama, J. Kucera, Y. Hirose and T. Amiya, *Nature*, 1987, 325, 796-798.

3 M.A. Biot, *Appl. Sci. Res.*, 1963, 12A, 168-182.

4 E. Matsuo and T. Tanaka, *Nature*, 1992, 358, 482-484.

5 B. Barrière, K. Sekimoto, and L. Leibler, *J. Chem. Phys.*, 1996, 105, 1735-1738.

6 S. Sasaki and H. Maeda, *J. Colloid Interface Sci.*, 1999, 211, 204-209

7 E.K. Rodriguez, A. Hoger, A. McCulloch, *J. Biomech.*, 1994, 27, 455-467

8 M. Ben Amar and P. Ciarletta, *J. Mech. Phys. Solids*, 2010, 58, 935-954.

9 H. Vaughan, *ZAMP*, 1971,22, 865-875

10 S. Mora, T. Phou, J.M. Fromental, L.M. Pismen, and Y. Pomeau, *Phys. Rev. Lett.*, 2010, 105, 214301

11 S. Ochs, R. Purmand, R.A. Jersild, R.N. Friedman *Progr. Neurobiol.*, 1997, 52, 391-426.

12 P. Ciarletta, I. Izzo, S. Micera, F. Tendick, 2011, *J. Mech. Behav. Biomed.*, 2011,4, 1359-1368.

13 R.A. Rvachev, *Biophys. Rev. Lett.*, 2010, 5, 73-88.

14 A. Boudaoud and S. Chaieb, *Phys. Rev. E*, 2003, 68, 021801

15 H. Fong, I. Chung and D.H. Reneker, *Polymer*, 1999, 40, 4585-4592